Morrissey, J. H. (1981) *Anal. Biochem. 117*, 307.
Nir, S., Stegmann, T., & Wilschut, J. (1986) *Biochemistry 25*, 257.
Oxford, J. S., Hockley, D. J., Heath, T. D., & Patterson, S. (1981) *J. Gen. Virol. 52*, 329.
Patzer, E. J., Wagner, R. R., & Dubovi, E. J. (1979) *CRC Crit. Rev. Biochem. 6*, 165.
Rouser, G., Kritchevsky, C., & Yamamoto, A. (1967) in *Lipid Chromatographic Analysis* (Marinetti, G. V., Ed.) Vol. 1, pp 99–162, Marcel Dekker, New York.
Salk, J. E. (1944) *J. Immunol. 49*, 87.
Sandermann, H. (1986) in *Progress in Protein–Lipid Interactions* (Watts, A., & de Pont, J. J. H. H. M., Eds.) Vol. 2, Elsevier, New York.
Skehel, J. J., Bayley, P. M., Brown, E. B., Martin, S. R., Waterfield, M. D., White, J. M., Wilson, I. A., & Wiley, D. C. (1982) *Proc. Natl. Acad. Sci. U.S.A. 79*, 968.
Stegmann, T., Hoekstra, D., Scherphof, G., & Wilschut, J. (1985) *Biochemistry 24*, 3107.
Tiffany, J. M., & Blough, H. A. (1969) *Science (Washington, D.C.) 163*, 573.
Warren, L. (1959) *J. Biol. Chem. 234*, 1971.
Wilschut, J., Duzgunes, N., Fraley, R., & Papahadjopoulos, D. (1980) *Biochemistry 19*, 6011.
Zacharius, R. M., Zell, T. E., Morrison, J. H., & Woodlock, J. J. (1969) *Anal. Biochem. 30*, 148.

Equilibrium and Dynamic Structure of Large, Unilamellar, Unsaturated Acyl Chain Phosphatidylcholine Vesicles. Higher Order Analysis of 1,6-Diphenyl-1,3,5-hexatriene and 1-[4-(Trimethylammonio)phenyl]-6-phenyl-1,3,5-hexatriene Anisotropy Decay†

Martin Straume‡ and Burton J. Litman*
Department of Biochemistry, University of Virginia School of Medicine, Charlottesville, Virginia 22908
Received November 4, 1986; Revised Manuscript Received March 31, 1987

ABSTRACT: Equilibrium and dynamic structural properties of minimally to highly unsaturated acyl chain, large, unilamellar phosphatidylcholine (PC) vesicles have been characterized by the dynamic fluorescence properties of 1,6-diphenyl-1,3,5-hexatriene (DPH) and 1-[4-(trimethylammonio)phenyl]-6-phenyl-1,3,5-hexatriene (TMA-DPH). Fluorescence lifetimes and equilibrium and dynamic rotational properties of these probes were analyzed by limited-frequency phase-modulation fluorometry in egg PC, palmitoyloleoyl-PC (POPC), dioleoyl-PC (DOPC), palmitoylarachidonoyl-PC (PAPC), and palmitoyldocosahexaenoyl-PC (P-22:6-PC) vesicles over a temperature range from 5 to 37 °C. DPH equilibrium orientational distributions were derived according to a model permitting bimodal orientational distributions in which the parallel probability maximum was aligned parallel to the bilayer normal and the orthogonal probability maximum was oriented parallel to the plane of the bilayer. TMA-DPH orientational distributions were derived according to the same model except that all probability was constrained to the parallel orientation. TMA-DPH fluorescence lifetimes were much more sensitive than those of DPH to variations in acyl chain composition and temperature although the same qualitative behavior was generally observed with both probes. Greater acyl chain unsaturation and higher sample temperatures each gave rise to shorter lifetimes consistent with increased water penetrability into the bilayers. Equilibrium order of the hydrocarbon core (as probed by DPH) and of the interfacial and head group regions of the bilayers (as probed by TMA-DPH) was reduced by increasing levels of unsaturation and by higher sample temperatures. The proportion of DPH in the orthogonal orientation increased with greater unsaturation and higher temperatures, indicative of more disorder of acyl chain termini under such conditions. Both probes exhibited accelerated rates of depolarization as temperatures were increased. Rates of DPH depolarizing motion were very similar to those of TMA-DPH at any given temperature.

Model lipid vesicle systems have routinely been used to characterize the physical properties of lipid bilayers as a function of molecular composition. Lipid vesicles may be prepared with defined composition to permit the study of systems that lack the great compositional heterogeneity present in natural biological membranes (Akino & Tsuda, 1979; Benga & Holmes, 1984; Miljanich et al., 1979; Thompson & Huang, 1986). Knowledge of the dependence of lipid physical properties on compositional variation has implications in understanding the nature of lipid–protein interactions and their involvement in mediating membrane-associated functions (Applebury et al., 1974; Baldwin & Hubbell, 1984a,b; Deese et al., 1981; Devaux & Seigneuret, 1985; Jahnig et al., 1982; Litman et al., 1981; O'Brien et al., 1977; Salesse & Garnier, 1984; Stubbs & Litman, 1978; Stubbs et al., 1976). Early work in this area has concentrated on studies of saturated acyl chain phospholipid vesicles. Biological membranes, however, contain substantial and varying proportions of unsaturated acyl chains (Akino & Tsuda, 1979; Benga & Holmes, 1984; Miljanich et al., 1979; Thompson & Huang, 1986). It is

†Supported by National Science Foundation Grant PCM-8316858 and National Institutes of Health Grant EY00548. A preliminary account of this work was presented at the annual meeting of the Biophysical Society, February 1986.
‡Present address: Department of Pharmacology, University of Virginia School of Medicine, Charlottesville, VA 22908.

0006-2960/87/0426-5113$01.50/0

therefore of importance to study the physical properties of unsaturated acyl chain, model vesicle systems.

Lipid molecular dynamics occur on the time scale of nanoseconds at physiological temperatures (Benga & Holmes, 1984; Brown & Williams, 1985; Devaux & Seigneuret, 1985; Stubbs, 1983; Thompson & Huang, 1986; Wong, 1984; Yeagle, 1984). Fluorescence techniques are particularly suitable for characterization of dynamic phenomena in this time domain because fluorescence lifetimes are generally in the range of nanoseconds to tens of nanoseconds (Lakowicz, 1983, 1981, 1980). Determination of the equilibrium and dynamic rotational properties of bilayer probes, as well as of their fluorescence intensity decay kinetics, allows information to be derived about fluorophore motional properties. Thus, by inference, information about the physical properties of the fluorophore environment may be ascertained. The fluorescent probes DPH[1] and TMA-DPH survey two different bilayer environments. DPH partitions into the hydrophobic core of lipid bilayers (Shinitzky & Barenholz, 1978) whereas the amphipathic TMA-DPH molecules reside in the interfacial and head group regions of membranes (Engel & Prendergast, 1981; Prendergast et al., 1981). Both probes exhibit very high intrinsic molecular anisotropy, facilitating sensitive detection of rotational phenomena. This sensitivity is necessary for characterizing liquid-crystalline bilayers due to the presence of only subtle variations in equilibrium probe orientational properties among such systems (Stubbs et al., 1981).

This paper applies a more advanced model to interpret anisotropy decay of DPH and TMA-DPH than has previously been employed. A bimodal orientational distribution, based on work by Ameloot et al. (1984) and van der Meer et al. (1984), is invoked to characterize DPH orientational distributions. Support for such a distribution of DPH in liquid-crystalline bilayers exists from steady-state experiments on oriented, planar bilayers (van de Ven et al., 1984; Vogel & Jahnig, 1985; Vos et al., 1983). Analysis of TMA-DPH orientational distributions is accomplished by employing the same model but constraining the distribution function to allow only one orientational probability maximum (Ameloot et al., 1984). The model thus restricts TMA-DPH molecules to an orientation parallel to the plane of the bilayer.

Experimental Procedures

Lipid Vesicle Preparation. Large, unilamellar phosphatidylcholine vesicles were prepared by an octyl glucoside dialysis method as described by Jackson et al. (1982) with the modifications described. Egg PC, POPC, DOPC, PAPC, and P-22:6-PC were obtained from Avanti Polar Lipids as chloroform solutions and used without further purification. Representative lots of lipids were checked for purity by thin-layer chromatography. All lipids were stored at −80 °C until used. PAPC and P-22:6-PC were used directly from the vials in which they came to reduce the likelihood of oxidation of arachidonoyl (20:4) and docosahexaenoyl (22:6) fatty acyl chains. Stock solutions of egg PC, POPC, and DOPC at approximately 50 mM lipid concentration were prepared by appropriate dilution of the original lipid solution into chloroform. These stock PC solutions were stored under Ar or N_2 at −20 °C.

Aliquots of lipid solutions were evaporated to dryness in lyophilization tubes under an Ar or N_2 atmosphere. To minimize oxidation of P-22:6-PC, dry BHT was added to lyophilization tubes prior to addition of this lipid to yield 0.1 mol % BHT relative to phospholipid. The dried lipid film was then redissolved in cyclohexane, frozen, and lyophilized overnight in the dark.

After lyophilization, the lipid was maintained under Ar or N_2 and dissolved in 100 mM OG in 50 mM Tris–acetate, 50 μM DTPA, 62.5 μM $MgCl_2$, pH 7, buffer (OG/T–A buffer). DTPA was included in the buffer to chelate any trace levels of soluble iron, a catalyst for lipid peroxidation, in order to reduce acyl side chain peroxidation. The T–A buffer was extensively degassed with Ar or N_2 prior to dissolving the OG. The OG/T–A buffer was then kept under Ar or N_2 at 4 °C until used. Lyophilized lipid was solubilized in cold, degassed OG/T–A buffer, and solubilization was allowed to proceed for 60–120 min under Ar or N_2 at 4 °C.

The OG/T–A/lipid solution was then dialyzed against three to four changes of a large excess of degassed T–A buffer for 36–48 h under Ar or N_2 at 4 °C. After dialysis, vesicles were stored under Ar or N_2 at 4 °C.

Total phospholipid concentration was determined by phosphate analysis according to the method of Bartlett (1959).

The extent of lipid peroxidation of PAPC and P-22:6-PC lipids was determined by both 233-nm absorbance and thiobarbituric acid assay (Baker & Wilson, 1966; Slater, 1984; Sunamoto et al., 1985). Peroxidation of PAPC was no greater than 0.5%, and that of P-22:6-PC was no greater than 2–3%.

Fluorescence Measurements. Aliquots of stock vesicle preparations were diluted to 3.0 mL of 0.5 mM P_i with degassed T–A buffer in stoppered fluorescence cuvettes. The cuvettes were flushed with Ar or N_2 prior to and during loading. Samples were then maintained under an inert atmosphere.

Diluted samples in cuvettes were labeled with DPH (in THF) or TMA-DPH (in DMF) to yield lipid:probe ratios of approximately 500:1 for DPH or approximately 250:1 for TMA-DPH (DPH and TMA-DPH were obtained from Molecular Probes). Labeling was accomplished by adding a few microliters of an approximately 2 mM stock probe solution to samples. Stock probe solutions were stored under Ar or N_2 at −20 °C. Labeled samples were sealed under Ar or N_2 in stoppered cuvettes.

Samples were loaded into the thermostated sample chamber of an SLM 4800 phase-modulation spectrofluorometer. Equilibration was allowed to proceed for at least 60 min at 37 °C with stirring. Small stir bars were placed into the cuvettes prior to loading of samples, and stirring was maintained throughout all measurements by way of a magnetic stirrer assembly mounted under the sample chamber. Temperature was controlled by a circulating water bath and detected by a thermistor located in an aluminum block in one of the four sample chamber positions.

Fluorescence excitation was accomplished by using a 500-W xenon arc lamp as a source and passing the light through a dual-grating monochromator set to 360 nm (1-nm band-pass). Fluorescence emission was detected after emitted light passed through a dual-grating monochromator set to 430 nm (16-nm band-pass).

A POPOP–absolute ethanol reference solution was used to optimize all optical and modulation tank settings and was also

[1] Abbreviations: DPH, 1,6-diphenyl-1,3,5-hexatriene; TMA-DPH, 1-[4-(trimethylammonio)phenyl]-6-phenyl-1,3,5-hexatriene; POPOP, 1,4-bis(5-phenyloxazol-2-yl)benzene; PC, phosphatidylcholine; egg PC, egg phosphatidylcholine; POPC, palmitoyloleoylphosphatidylcholine; DOPC, dioleoylphosphatidylcholine; PAPC, palmitoylarachidonoylphosphatidylcholine; P-22:6-PC, palmitoyldocosahexaenoylphosphatidylcholine; OG, octyl β-D-glucoside; Tris, tris(hydroxymethyl)aminomethane; DTPA, diethylenetriaminepentaacetate; BHT, butylated hydroxytoluene; THF, tetrahydrofuran; DMF, dimethylformamide; P_i, inorganic phosphate; NMR, nuclear magnetic resonance.

used as a dynamic fluorescence reference. POPOP in absolute ethanol exhibits a fluorescence lifetime of 1.35 ns, which is independent of temperature over the range used in this work, and has excitation and emission spectra compatible with the wavelengths of excitation and emission of DPH and TMA-DPH (Lakowicz et al., 1981). Use of such a dynamic fluorescence reference solution eliminates potential geometric and color effects that are possible with the use of a scattering reference suspension (Lakowicz et al., 1981).

To characterize the fluorescence lifetime, equilibrium order, and rotational dynamics of DPH and TMA-DPH in lipid bilayers, a number of independent equilibrium and dynamic fluorescence parameters were determined.

The steady-state fluorescence anisotropy r_s is defined as

$$r_s = (I_\parallel - I_\perp)/(I_\parallel + 2I_\perp) = (R - 1)/(R + 2)$$

where $R = I_\parallel/I_\perp$. R is observed experimentally as

$$R = I_{VV}I_{HH}/I_{VH}I_{HV}$$

where $I_{i,j}$ is defined as the fluorescence intensity with the excitation polarizer oriented in the i direction and the emission polarizer oriented in the j direction. The subscripts V and H indicate the vertical and horizontal polarizer orientations, respectively. The correction factor (I_{HH}/I_{HV}) is present to account for different efficiencies of detection of emitted fluorescence with respect to emission polarizer orientation. A further correction to R was found necessary when a solution of *N*-methylacridinium perchlorate in methanol at 20 °C was examined. This solution should exhibit an r_s of zero. It was found that our instrument required correction as

$$r_s = (R/1.04 - 1)/(R/1.04 + 2)$$

Dynamic phase-angle shifts and amplitude demodulations were determined for labeled vesicles relative to a POPOP–absolute ethanol reference solution. Given 1.35 ns as the fluorescence lifetime of this reference solution, absolute phase angles and modulation ratios of the fluorescence from labeled vesicles were calculated. Phase angles were determined at 30 and 6 MHz, and modulation ratios were determined at 30 MHz. Modulation ratios at 6 MHz were insensitive due to the short lifetimes encountered (<10 ns), and the 18-MHz modulation frequency was incapable of giving reliable phase-angle or demodulation information due to low absolute instrumental modulation at this frequency. All measurements of total fluorescence intensity decay parameters were made with a vertical excitation polarizer and an emission polarizer oriented 55° from the vertical (Lakowicz, 1983).

Differential phase angles were determined at 30 and 6 MHz by subtracting the phase angle observed with vertically polarized emission from that observed with horizontally polarized emission when samples were excited with vertically polarized light. Eighteen-megahertz differential phase angles were not employed in analysis because of unreliability due to low absolute instrumental modulation at this frequency.

A full set of steady-state and dynamic data was acquired at 37, 25, 15, and 5 °C for each sample after initial equilibration at 37 °C. Less than 1% background intensity was detected from unlabeled samples.

Methods of Analysis. Total fluorescence intensity decay behavior was fit to a constrained two-population model. Phase angles at 30 and 6 MHz and modulation ratios at 30 MHz were used to define the fractional amplitude α_i and lifetime τ_i parameters:

$$I_{tot}(t) = \sum_{i=1}^{2} \alpha_i \exp(-t/\tau_i)$$

$$\alpha_2 = 1 - \alpha_1 \qquad \tau_2 = 4\tau_1$$

The constraint defining the τ_2/τ_1 ratio was based on numerous reports in the literature supporting the validity of this approximate ratio of lifetimes for DPH in lipid bilayers [see, for example, Ameloot et al. (1984), Chen et al. (1977), Hildenbrand and Nicolau (1979), Kawato et al. (1977), Kinosita et al. (1981a,b), Klausner et al. (1980), Lakowicz et al. (1985), Parasassi et al. (1984), and Stubbs et al. (1984, 1981)].

The intensity-weighted mean fluorescence lifetime $\tau(1)$ is represented by

$$\tau(1) = (1/\langle\tau\rangle)\sum_{i=1}^{2}\alpha_i\tau_i^2 \qquad \langle\tau\rangle = \sum_{i=1}^{2}\alpha_i\tau_i$$

Equilibrium probe orientational distributions and rates of probe depolarizing motions were obtained by application of a model derived by van der Meer et al. (1984) that characterizes the kinetics of anisotropy decay. This model employs a higher order description of anisotropy decay (for rodlike fluorophores with collinear excitation, emission, and long molecular axes) than have earlier models. The expressions defining the time dependence of anisotropy $r(t)$ according to this model are

$$r(t) = b_4 + \sum_{j=1}^{3} b_j \exp(-t/\phi_j)$$

$$b_1 = r_0[1/5 + 2\langle P_2\rangle/7 + 18\langle P_4\rangle/35 - \langle P_2\rangle^2]$$

$$b_2 = 2r_0[1/5 + \langle P_2\rangle/7 - 12\langle P_4\rangle/35]$$

$$b_3 = 2r_0[1/5 - 2\langle P_2\rangle/7 + 3\langle P_4\rangle/35]$$

$$b_4 = r_0\langle P_2\rangle^2$$

$$\phi_1 = (b_1/6r_0D_\perp)[1/5 + \langle P_2\rangle/7 - 12\langle P_4\rangle/35]^{-1}$$

$$\phi_2 = (b_2/6r_0D_\perp)[1/5 + \langle P_2\rangle/14 + 8\langle P_4\rangle/35]^{-1}$$

$$\phi_3 = (b_3/12r_0D_\perp)[1/5 - \langle P_2\rangle/7 - 2\langle P_4\rangle/35]^{-1}$$

$$r_0 = 0.392$$

$$\langle P_2\rangle = (1/N)\int_0^\pi f(\theta)P_2(\cos\theta)\sin\theta\,d\theta$$

$$\langle P_4\rangle = (1/N)\int_0^\pi f(\theta)P_4(\cos\theta)\sin\theta\,d\theta$$

$$N = \int_0^\pi f(\theta)\sin\theta\,d\theta$$

$$P_2(\cos\theta) = (3\cos^2\theta - 1)/2$$

$$P_4(\cos\theta) = (35\cos^4\theta - 30\cos^2\theta + 3)/8$$

Knowledge of the equilibrium probe orientational distribution function $f(\theta)$ and the perpendicular rotational diffusion coefficient $D_\perp$ fully defines the anisotropy decay behavior. Work by Ameloot et al. (1984), van de Ven et al. (1984), Vogel and Jahnig (1985), and Vos et al. (1983) supports the existence of two orthogonal DPH distribution peaks in liquid-crystalline lipid bilayers. The form of $f(\theta)$ was therefore selected to be

$$f(\theta) = (\beta^2/2)\left\{\exp\left[-\left(\frac{\theta}{\theta_g}\right)^2\right] + \exp\left[-\left(\frac{\pi-\theta}{\theta_g}\right)^2\right]\right\} + (1-\beta)^2\exp\left\{-\left[\frac{(\pi/2)-\theta}{\theta_g}\right]^2\right\}$$

TMA-DPH distributions were fit to the same expression for $f(\theta)$ except that β was constrained to a value of 1. The re-

sulting equilibrium orientational distribution function did not allow any TMA-DPH molecules to occupy the orthogonal distribution peak. The TMA-DPH distribution was therefore constrained parallel to the phospholipid acyl chains. Experimental results of Ameloot et al. (1984) support the absence of any orthogonal TMA-DPH population in lipid vesicles. This is consistent with the intuitive expectation that no cationic TMA-DPH molecules should occupy the totally hydrophobic environment at the bilayer median.

The fraction of probe molecules parallel to the bilayer normal, i.e., parallel to the phospholipid acyl chains, is defined as

$$f_{\parallel} = (1/N)\int_0^{\pi} f_{\parallel}(\theta)\sin\theta\, d\theta$$

$$f_{\parallel}(\theta) = (\beta^2/2)\left\{\exp\left[-\left(\frac{\theta}{\theta_g}\right)^2\right] + \exp\left[-\left(\frac{\pi-\theta}{\theta_g}\right)^2\right]\right\}$$

In the case of TMA-DPH-labeled vesicles, $f_{\parallel}$ always equals 1.

The fractional volume available for probe reorientational motion, f_v, is defined as

$$f_v = (1/2f(\theta)_{max})\int_0^{\pi} f(\theta)\sin\theta\, d\theta$$

This parameter ranges in value from 0 to 1 and characterizes the volume available for probe reorientation relative to that available in a microscopically isotropic, unhindered probe environment. The fractional volume conveniently characterizes the overall equilibrium order detected by DPH or TMA-DPH.

All parameter and confidence interval estimation was performed by a modified Gauss–Newton, nonlinear least-squares procedure (Johnson, 1983; Johnson & Frasier, 1985).

Results

Fluorescence Lifetimes. The results of the constrained two-population fluorescence intensity decay analysis for DPH- and TMA-DPH-labeled vesicles indicate that the fractional amplitude of the short lifetime component α_1 usually corresponds to less than half of the excited fluorophores [see the supplementary material of Straume and Litman (1987)]. Short lifetime fractional amplitudes of 0.5 or less transform to fractional intensities of 0.2 or less for the short lifetime population when the ratio τ_2/τ_1 is constrained to a value of 4. The total fluorescence intensity decays observed for DPH- and TMA-DPH-labeled vesicles are therefore composed primarily of intensity arising from the derived long-lifetime fluorophore population.

The intensity-weighted mean fluorescence lifetime, $\tau(1)$, may be used for comparison of the average lifetime behavior of these fluorophores. The mean lifetime of DPH is much less sensitive than that of TMA-DPH to changes in acyl chain composition or sample temperature [see the supplementary material of Straume and Litman (1987)]. Temperature and acyl chain dependent variations of DPH lifetimes are therefore somewhat less consistent than are those of TMA-DPH, although the same general trends are qualitatively apparent. Both an increase in sample temperature and an increase in the degree of acyl chain unsaturation result in shorter mean fluorescence lifetimes. Figure 1 presents the $\tau(1)$ values derived for TMA-DPH-labeled vesicles at 37 and 5 °C.

Equilibrium Order. The Gaussian distribution widths θ_g derived for DPH are consistently narrower than those derived for TMA-DPH [see the supplementary material of Straume and Litman (1987)]. Both probes exhibit the same qualitative

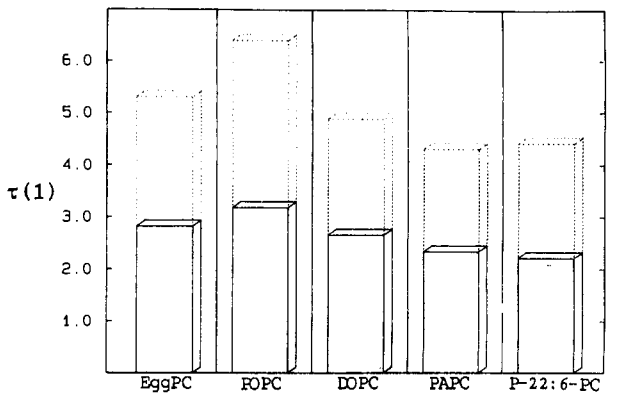

FIGURE 1: Intensity-weighted mean fluorescence lifetimes, $\tau(1)$ (in nanoseconds), of TMA-DPH-labeled vesicles. Solid lines, T = 37 °C; dotted lines, T = 5 °C.

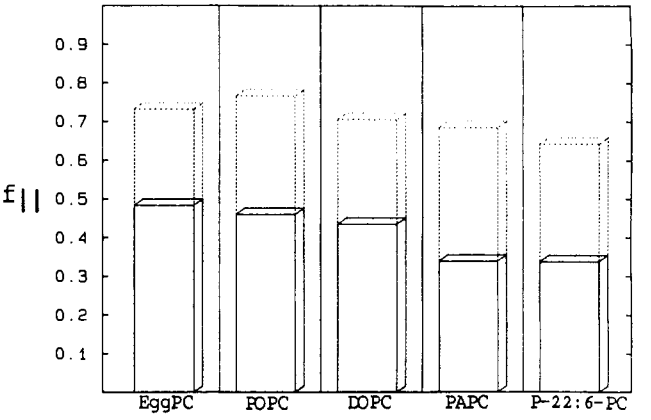

FIGURE 2: Fractions of DPH equilibrium orientational distributions aligned parallel to the bilayer normal, $f_{\parallel}$. Solid lines, T = 37 °C; dotted lines, T = 5 °C.

behavior of θ_g with respect to changes in sample temperature and acyl chain composition. Increases in either temperature or unsaturation contribute to broader derived equilibrium orientational distributions.

To fully define the DPH orientational distribution function, it is necessary to know the relative contributions of the two orthogonal probability maxima as well as the Gaussian distribution width. The fraction of DPH molecules parallel to the phospholipid acyl chains, $f_{\parallel}$, increases as the temperature or degree of acyl chain unsaturation is reduced [Figure 2; see the supplementary material of Straume and Litman (1987)]. Changes in temperature or acyl chain unsaturation therefore cause an orientational redistribution of DPH in these lipid bilayers.

The fractional volume available for probe reorientation relative to that available in a microscopically isotropic, unhindered probe environment, f_v, quantifies the overall equilibrium ordering detected by DPH or TMA-DPH. This parameter takes into account both $f_{\parallel}$ and θ_g, thereby obviating the need to consider these two parameters simultaneously. Direct comparisons between DPH and TMA-DPH results are thus possible as are comparisons among results obtained with DPH that differ in their $f_{\parallel}$ values. The equilibrium order detected by DPH is more sensitive to variations in sample temperature and acyl chain unsaturation than is that of TMA-DPH [Figure 3; see the supplementary material of Straume and Litman (1987)]. At high sample temperature (37 °C), f_v for DPH is greater than that for TMA-DPH, whereas at low sample temperature (5 °C), the fractional volume available to DPH is less than that available to TMA-DPH. Increasing sample temperature and increasing acyl

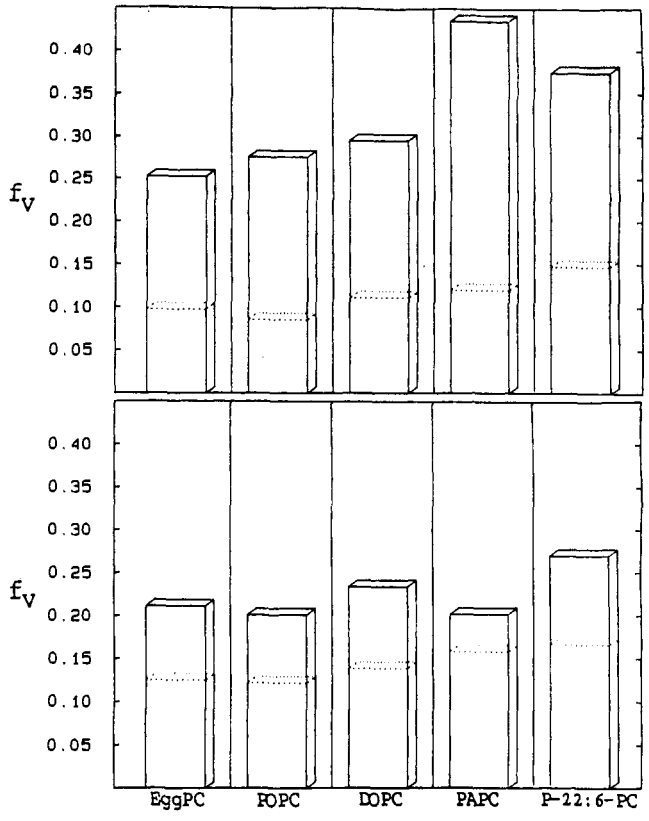

FIGURE 3: Fractional volumes, f_v, derived for DPH- (top) and TMA-DPH- (bottom) labeled vesicles. Solid lines, T = 37 °C; dotted lines, T = 5 °C.

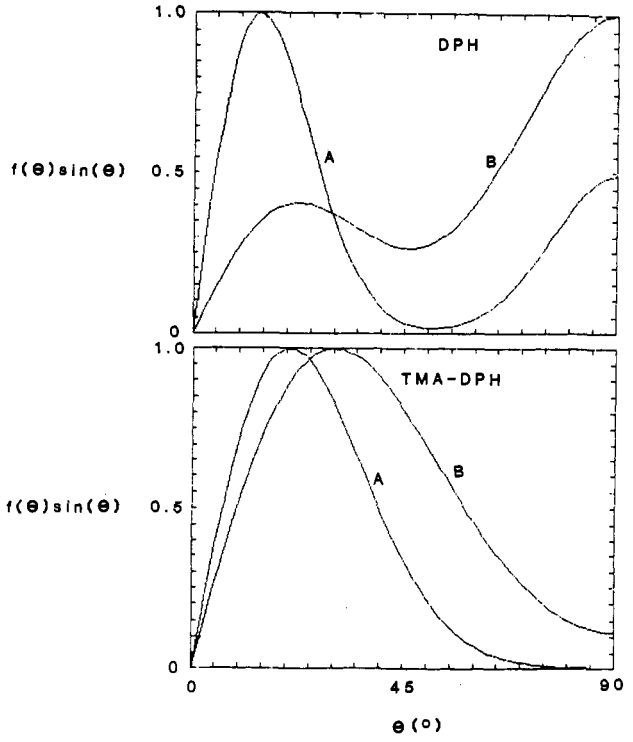

FIGURE 4: Equilibrium orientational distributions representative of the most ordered (A) and the most disordered (B) distributions derived for DPH- (top) and TMA-DPH- (bottom) labeled vesicles. DPH: (A) $\beta = 0.84$, $\theta_g = 20°$, $f_\parallel = 0.735$, $f_v = 0.081$; (B) $\beta = 0.65$, $\theta_g = 32°$, $f_\parallel = 0.358$, $f_v = 0.414$. TMA-DPH: (A) $\beta = 1.0$, $\theta_g = 30°$, $f_\parallel = 1.0$, $f_v = 0.131$; (B) $\beta = 1.0$, $\theta_g = 45°$, $f_\parallel = 1.0$, $f_v = 0.279$.

chain unsaturation each contribute to greater f_v values.

Rotational Dynamics. The perpendicular rotational diffusion coefficient, $D_\perp$, characterizes the rate of probe depolarizing motions. Each of the systems examined exhibits increased $D_\perp$ values with increases in sample temperature for both DPH and TMA-DPH [see the supplementary material of Straume and Litman (1987)]. TMA-DPH has values of $D_\perp$ in the range of approximately 0.12–0.14 ns^{-1} at 5 °C that increase to approximately 0.25–0.52 ns^{-1} at 37 °C. Values of $D_\perp$ for DPH range from approximately 0.12–0.18 ns^{-1} at 5 °C to approximately 0.24–0.42 ns^{-1} at 37 °C.

Discussion

The use of fluorescent probes to characterize lipid membrane systems provides an extremely sensitive method for detection of equilibrium and dynamic structural properties of bilayers on the time scale of nanoseconds. The implicit assumptions underlying such experiments are (1) that the probes accurately report about the equilibrium and dynamic structural properties of local environments within bilayers and (2) that they induce no significant perturbation to the system under study by their presence.

In this paper, the dynamic fluorescence properties of DPH and TMA-DPH in minimally to highly unsaturated, large, unilamellar phosphatidylcholine vesicles are characterized by a higher order analysis of anisotropy decay. Previous models have assumed unimodal DPH orientational probability distributions centered about the bilayer normal (Engel & Prendergast, 1981; Kinosita et al., 1977). A model advanced by van der Meer et al. (1984) permits characterization so as to accommodate more complex equilibrium orientational distributions. Dynamic studies conducted by Ameloot et al. (1984) and steady-state experiments performed on oriented, planar bilayers (van de Ven et al., 1984; Vogel & Jahnig, 1985; Vos et al., 1983) support the existence of orthogonal, bimodal distributions of DPH in liquid-crystalline bilayers. TMA-DPH, however, appears to exhibit only a unimodal distribution with maximum probability centered about the bilayer normal (Ameloot et al., 1984).

This paper employs a distribution function with Gaussian, orthogonal probability maxima of equivalent width. Figure 4 presents plots of the distribution functions for DPH and TMA-DPH characteristic of the most ordered and the most disordered distributions derived for each of these probes in this paper. A considerable proportion of DPH may occupy a distribution at the median of the bilayer, oriented parallel to the bilayer plane (at $\theta = 90°$).

Total probe fluorescence intensity decay kinetics determined by measurements at only a few modulation frequencies required the imposition of a constraint in the discrete two-population model employed for analysis. On the basis of previously reported total intensity decay behavior for DPH in lipid vesicles, the long lifetime is constrained to a value 4 times that of the short lifetime (Ameloot et al., 1984; Chen et al., 1977; Hildenbrand & Nicolau, 1979; Kawato et al., 1977; Kinosita et al., 1981a,b; Klausner et al., 1980; Lakowicz et al., 1985; Parasassi et al., 1984; Stubbs et al., 1984, 1981). This constraint permits consistent convergence to physically reasonable results that agree well with behavior reported previously (Stubbs et al., 1981). The same constraint is employed in analysis of TMA-DPH total intensity decays.

Primarily long-lifetime fluorophores account for the observed intensity decays regardless of sample temperature for both DPH and TMA-DPH in the vesicles examined. The two-population model employed is meant only to better approximate intensity decay kinetics than does a monoexponential model. The actual intensity decay is almost certainly characterized by continuous distributions of fluorophore lifetimes (Glaser et al., 1986). A precise interpretation of derived α_i

and τ_i parameters is therefore not possible. They are model-dependent, derived parameters characteristic of an approximation to the distribution of probe lifetimes present in the observed systems.

Fluorescence intensity decay kinetics may be compared by observing changes in the intensity-weighted mean fluorescence lifetimes, $\tau(1)$, characteristic of the average probe exicted-state lifetimes. DPH mean lifetimes are considerably less sensitive to variations in acyl chain composition and sample temperature than are those of TMA-DPH. This may be accounted for by the different locations of DPH and TMA-DPH in bilayers. DPH localizes in the hydrocarbon core of lipid bilayers (Lakowicz, 1983; Shinitzky & Barenholz, 1978) whereas TMA-DPH resides at the bilayer head group and interfacial regions (Ameloot et al., 1984; Engel & Prendergast, 1981; Prendergast et al., 1981). TMA-DPH is therefore more likely to experience quenching by probe–water interactions than is DPH.

Greater unsaturation and higher sample temperatures result in shorter mean lifetimes, suggesting that greater equilibrium and/or dynamic molecular disorder is present which increases the probability of water penetration into the bilayer structure. Dynamic quenching of probe fluorescence by probe–water interactions may thus lead to reduced fluorescence lifetimes under conditions that promote water transport into bilayers. The occurrence and migration of β-coupled gauche-trans-gauche conformations along phospholipid acyl chains may be a mechanism permitting the transport of water into bilayers (Thompson & Huang, 1986). ^{1}H NMR results suggest that gauche-trans conformational changes occur on the nanosecond time scale (Horwitz et al., 1972), and dynamic PC head group fluctuations have also been shown to occur on this time scale by ^{1}H–^{31}P nuclear Overhauser studies (Yeagle et al., 1975). Elevated temperatures will accelerate both head group dynamics and the frequency of gauche-trans conformational fluctuations as a result of increased molecular energy content. Acyl chain unsaturation reduces the energy barrier for rotation about C–C bonds adjacent to double bonds (Thompson & Huang, 1986), and acyl chain mobility is increased with greater unsaturation (Barton & Gunstone, 1975; Kohler et al., 1972). In addition, greater unsaturation promotes weaker head group–head group interactions (Jendrasiak & Hasty, 1974a,b), resulting in greater effective head group volume (Demel et al., 1972; Ghosh et al., 1973) and more head group mobility (Levine et al., 1972). These phenomena are expected to facilitate the penetration of water into lipid bilayers and are consistent with reduced fluorescence lifetimes in the more highly unsaturated systems examined. Migration of β-coupled gauche-trans-gauche conformations is largely restricted to the carbonyl end of phospholipid acyl chains whereas independent C–C rotations dominate nearer the methyl termini (Edholm, 1981). Transport of water into bilayers by migration of such coupled conformations is consistent with the greater sensitivity of TMA-DPH lifetimes than of those of DPH to variations in temperature and acyl chain unsaturation.

The derived distribution widths, θ_g, for DPH are consistently narrower than those derived for equivalent systems labeled with TMA-DPH. This is consistent with the presence of an extra degree of freedom available for DPH reorientational motion relative to that for TMA-DPH. TMA-DPH is constrained by a permanent positive charge at one end of this rodlike molecule to reorient within a single orientational probability maximum parallel to the bilayer normal. DPH, however, is free to occupy two orthogonal probability maxima, one parallel to the bilayer normal and the other within the plane of the bilayer. The freedom available to DPH to rapidly exchange between these two orthogonal distributions permits DPH molecules to accommodate their reorientational energy by an additional mode of rotational relaxation. Thus, DPH may occupy a free volume roughly equivalent to that experienced by TMA-DPH by maintaining narrower individual distribution peaks but varying the relative contributions of the two orthogonal probability maxima.

Broader derived distribution widths for DPH and TMA-DPH as sample temperature or acyl chain unsaturation is increased imply greater equilibrium freedom for molecular motions both at the bilayer hydrocarbon core and at the interfacial and head group regions. ^{1}H and ^{13}C NMR studies support that greater bilayer unstaturation leads to enhanced mobility of phospholipid acyl chains (Barton & Gustone, 1975; Kohler et al., 1972) and to increased head group mobility, hydration, and effective volume (Demel et al., 1972; Ghosh et al., 1973; Jendrasiak & Hasty, 1974a,b; Levine et al., 1972). Elevated temperatures will increase the extent of molecular fluctuations in all regions of the bilayers and thus allow for broader probe orientational distributions for both DPH and TMA-DPH.

In the case of DPH-labeled vesicles, greater acyl chain unsaturation and increased sample temperatures both contribute to an increased proportion of orthogonally oriented probes. This result suggests that the acyl chain terminal region in the bilayer interior is more disordered under conditions of higher temperature or greater levels of unsaturation. Evidence exists supporting the presence of a mobility gradient in which progressively more motional freedom exists nearer the acyl chain methyl termini than at their carbonyl attachment sites to the phospholipid glycerol backbone (Brown & Williams, 1985; Davis, 1983; Lee, 1975). Acyl chain methyl-terminal regions would thus be expected to experience the most enhanced motional freedom in response to increased acyl chain unsaturation and elevated temperatures.

Estimates of average equilibrium ordering detected by either DPH or TMA-DPH are conveniently represented by the fractional volume available for probe reorientation, f_v. Both the hydrocarbon core and the interfacial and head group regions of these vesicles accommodate greater probe fractional volumes as either temperature or acyl chain unsaturation is increased. The ordering of the bilayer interior, however, is more sensitive than is that of the bilayer–water interface. Much of this may be related to the greater freedom for molecular motions available at the methyl termini of acyl chains relative to that nearer the bilayer–water interface (Brown & Williams, 1985; Davis, 1983 Lee, 1975). The greater sensitivity of DPH fractional volumes than of those of TMA-DPH suggests that the hydrocarbon core of vesicles is capable of varying its local molecular packing density over a wider range than may the bilayer–water interfacial region of liquid-crystalline, unsaturated acyl chain PC bilayers.

Rates of DPH and TMA-DPH depolarizing motions are accelerated by increasing temperature, suggesting more rapid bilayer dynamics at higher temperatures both in the hydrocarbon core and at the head group and interfacial regions of these vesicles. However, rates of molecular motion are approximately the same at the bilayer–water interface and in the hydrocarbon core. These results are in contrast to dynamic parameters reported by NMR studies that suggest sensitivity of molecular dynamics to depth within the bilayer (Brown & Williams, 1985; Lee, 1975; Levine et al., 1972). This difference may be related to the much larger reporter group used in these fluorescence studies vs. that observed in NMR experiments. Detection of highly localized phenomena, as in

NMR experiments, will minimize the range of bilayer physical properties experienced and averaged in a single, reported structural parameter. Fluorescent probes, on the other hand, are expected to experience a much broader distribution of equilibrium and dynamic structural states resulting in less sensitivity in detecting highly localized phenomena. When comparing results from different physical techniques, it is important to bear in mind any differences in time scales that may exist in the phenomena being detected. Fluorescent techniques generally detect phenomena occurring within the nanosecond time domain whereas NMR may detect molecular dynamics on the same time scale or up to 4 orders of magnitude more slowly. It is therefore necessary to define the terms "equilibrium" and "dynamic" in the context of appropriate frequency domains.

The trends in the derived fluorophore properties as a function of acyl chain unsaturation are relatively subtle compared to the more substantial differences observed between gel and liquid-crystalline bilayers (Lakowicz, 1983, 1981, 1980; Lakowicz & Prendergast, 1978; Lakowicz et al., 1979; Shinitzky & Barenholz, 1978). It is of interest to characterize the properties of unsaturated acyl chain phospholipids because of the significant proportions of unsaturated acyl chains found in biological membranes (Akino & Tsuda, 1979; Benga & Holmes, 1984; Miljanich et al., 1979; Thompson & Huang, 1986). Some specialized membrane systems, for example, rod outer segment disk membranes and the membranes of electric organs of electric fishes, contain up to 50% docosahexaenoyl (22:6) fatty acyl chains (Anderson & Maude, 1970; Anderson & Sperling, 1971; Borggreven et al., 1970; Gonzalez-Roz et al., 1982; Miljanich et al., 1979; Nielsen et al., 1970; Poincelot & Abrahamson, 1970; Popot et al., 1978). Therefore, although the trends detected are relatively subtle, these differences in physical properties may be involved in modulation of equilibrium and dynamic structural properties of membrane-associated proteins that regulate functional responses (Applebury et al., 1974; Baldwin & Hubbell, 1985a,b; Lewis et al., 1981; Litman et al., 1981; Morton et al., 1986; O'Brien et al., 1977; Stubbs & Litman, 1978).

Application of a bimodal orientational distribution function in analysis of the dynamics of DPH depolarization allows more detailed interpretation of probe reorientational phenomena. It should be pointed out, however, that two other alternative models have recently been proposed. In both cases, two populations of rotational species differing in their rates and extents of depolarization are assumed. In the model applied by Wang et al. (1986), total fluorescence intensity decay kinetics are analyzed according to a biexponential function. Subsequent analysis of rotational dynamics involves associating individual rotational correlation times and maximal extents of depolarization of each of these two derived fluorophore populations. An analysis employed by Davenport et al. (1986) is similar to that of Wang et al. (1986) except that each of the two derived rotational populations share common total fluorescence intensity decay properties. A common feature shared by the bimodal form of analysis and the analyses employed by Wang et al. (1986) and Davenport et al. (1986) is that more degrees of freedom are available in analysis to better accommodate the precise dynamics of DPH anisotropy decay than were available in less complex earlier models that were commonly employed.

Independent of this abundance of different analytical models, the bimodal analysis applied to DPH in addition to the characterization of TMA-DPH in the unsaturated PC vesicles examined in this paper provides new insight into subtle equilibrium and dynamic structural variations as a function of acyl chain composition, temperature, and location within the bilayer. The following paper (Straume & Litman, 1987) deals with an examination of the effects of cholesterol on the physical properties of the PC vesicle systems examined here by application of the same experimental and analytical methods.

ACKNOWLEDGMENTS

We thank Dr. M. L. Johnson for providing general-purpose software and assistance in nonlinear least-squares analysis. We also thank J. Murphy and Dr. M. L. Jackson for technical assistance and expertise in preparation of some of the samples.

REFERENCES

Akino, T., & Tsuda, M. (1979) *Biochim. Biophys. Acta 556*, 61–71.

Ameloot, M., Hendrickx, H., Herreman, W., Pottel, H., van Cauwelaert, F., & van der Meer, W. (1984) *Biophys. J. 46*, 525–539.

Anderson, R. E., & Maude, M. B. (1970) *Biochemistry 9*, 3624–3628.

Anderson, R. E., & Sperling, L. (1971) *Arch. Biochem. Biophys. 144*, 673–677.

Applebury, M. L., Zuckerman, D. M., Lamola, A. A., & Jovin, T. M. (1974) *Biochemistry 13*, 3448–3458.

Baker, N., & Wilson, L. (1966) *J. Lipid Res. 7*, 341–348.

Baldwin, P. A., & Hubbell, W. L. (1985a) *Biochemistry 24*, 2624–2632.

Baldwin, P. A., & Hubbell, W. L. (1985b) *Biochemistry 24*, 2633–2639.

Bartlett, G. R. (1959) *J. Biol. Chem. 234*, 466–468.

Barton, P. G., & Gunstone, F. D. (1975) *J. Biol. Chem. 256*, 4470–4476.

Benga, G., & Holmes, R. P. (1984) *Prog. Biophys. Mol. Biol. 43*, 195–257.

Borggreven, J. M. P. M., Daemen, F. J. M., & Bonting, S. L. (1970) *Biochim. Biophys. Acta 202*, 374–381.

Brown, M. F., & Williams, G. D. (1985) *J. Biochem. Biophys. Methods 11*, 71–81.

Chen, L. A., Dale, R. E., Roth, S., & Brand, L. (1977) *J. Biol. Chem. 252*, 2163–2169.

Davenport, L., Knutson, J. R., & Brand, L. (1986) *Biochemistry 25*, 1811–1816.

Davis, J. H. (1983) *Biochim. Biophys. Acta 737*, 117–171.

Deese, A. J., Dratz, E. A., Dahlquist, F. W., & Paddy, M. R. (1981) *Biochemistry 20*, 6420–6427.

Demel, R. A., Bruckdorfer, K. R., & van Deenen, L. L. M. (1972) *Biochim. Biophys. Acta 255*, 321–330.

Devaux, P. F., & Seigneuret, M. (1985) *Biochim. Biophys. Acta 822*, 63–125.

Edholm, O. (1981) *Chem. Phys. Lipids 29*, 213–224.

Engel, L. W., & Prendergast, F. G. (1981) *Biochemistry 20*, 7338–7345.

Ghosh, D., Williams, M. A., & Tinoco, J. (1973) *Biochim. Biophys. Acta 291*, 351–362.

Glaser, M., Fiorini, R., Wang, S., Valentino, M., & Gratton, E. (1986) *Biophys. J. 49*, 307a.

Gonzalez-Ros, J. M., Llanillo, M., Paraschosa, A., & Martinez-Carrion, M. (1982) *Biochemistry 21*, 3467–3474.

Hildenbrand, K., & Nicolau, C. (1979) *Biochim. Biophys. Acta 553*, 365–377.

Horwitz, A. F., Lein, M. P., Michaelson, D. M., & Kohler, S. J. (1972) *Ann. N.Y. Acad. Sci. 222*, 468–487.

Jackson, M. L., Schmidt, C. F., Lichtenberg, D., Litman, B. J., & Albert, A. D. (1982) *Biochemistry 21*, 4576–4582.

Jahnig, F., Vogel, H., & Best, L. (1982) *Biochemistry 21*, 6790–6798.
Jendrasiak, G. L., & Hasty, J. H. (1974a) *Biochim. Biophys. Acta 348*, 45–54.
Jendrasiak, G. L., & Hasty, J. H. (1974b) *Biochim. Biophys. Acta 337*, 79–91.
Johnson, M. L. (1983) *Biophys. J. 44*, 101–106.
Johnson, M. L., & Frasier, S. G. (1985) *Methods Enzymol. 117*, 301–342.
Kawato, S., Kinosita, K., Jr., & Ikegami, A. (1977) *Biochemistry 16*, 2319–2324.
Kinosita, K., Jr., Kawato, S., & Ikegami, A. (1977) *Biophys. J. 20*, 289–305.
Kinosita, K., Jr., Kataoka, R., Kimura, Y., Gotoh, O., & Ikegami, A. (1981a) *Biochemistry 20*, 4270–4277.
Kinosita, K., Jr., Kawato, S., Ikegami, A., Yoshida, S., & Orii, Y. (1981b) *Biochim. Biophys. Acta 647*, 7–17.
Klausner, R. D., Kleinfeld, A. M., Hoover, R. L., & Karnovsky, M. J. (1980) *J. Biol. Chem. 255*, 1286–1295.
Kohler, S. J., Horwitz, A. F., & Klein, M. P. (1972) *Biochem. Biophys. Res. Commun. 49*, 1414–1421.
Lakowicz, J. R. (1980) *J. Biochem. Biophys. Methods 2*, 91–119.
Lakowicz, J. R. (1981) in *Spectroscopy in Biochemistry* (Bell, J. Ellis, Ed.) pp 195–245, CRC Press, Boca Raton, FL.
Lakowicz, J. R. (1983) *Principles of Fluorescence Spectroscopy*, Plenum, New York.
Lakowicz, J. R., & Prendergast, F. G. (1978) *Science (Washington, D.C.) 200*, 1399–1401.
Lakowicz, J. R., Prendergast, F. G., & Hogan, D. (1979) *Biochemistry 18*, 508–519.
Lakowicz, J. R., Cherek, H., & Balter, A. (1981) *J. Biochem. Biophys. Methods 5*, 131–146.
Lakowicz, J. R., Cherek, H., Maliwal, B. P., & Gratton, E. (1985) *Biochemistry 24*, 376–383.
Lee, A. G. (1975) *Prog. Biophys. Mol. Biol. 29*, 3–56.
Levine, Y. K., Birdsall, N. J. M., Lee, A. G., & Metcalfe, J. C. (1972) *Biochemistry 11*, 1416–1421.
Lewis, J. W., Winterle, J. S., Powers, M. A., Kliger, D. S., & Dratz, E. A. (1981) *Photochem. Photobiol. 34*, 375–384.
Litman, B. J., Kalisky, O., & Ottolenghi, M. (1981) *Biochemistry 20*, 631–634.
Miljanich, G. P., Sklar, L. A., White, D. L., & Dratz, E. A. (1979) *Biochim. Biophys. Acta 552*, 294–306.
Morton, R. W., Straume, M., Miller, J. L., & Litman, B. J. (1986) *Biophys. J. 49*, 277a.
Nielsen, N. C., Fleischer, S., & McConnell, D. G. (1970) *Biochim. Biophys. Acta 211*, 10–19.
O'Brien, D. F., Costa, L. F., & Ott, R. A. (1977) *Biochemistry 16*, 1295–1303.
Parasassi, T., Conti, F., Glaser, M., & Gratton, E. (1984) *J. Biol. Chem. 259*, 14011–14017.
Poincelot, R. P., & Abrahamson, E. W. (1970) *Biochemistry 9*, 1820–1825.
Popot, J. L., Demel, R. A., Sobel, A., van Deenen, L. L. M., & Changeaux, J.-P. (1978) *Eur. J. Biochem. 85*, 27–42.
Prendergast, F. G., Haugland, R. P., & Callahan, P. J. (1981) *Biochemistry 20*, 7333–7338.
Salesse, R., & Garnier, J. (1984) *Mol. Cell. Biochem. 60*, 17–31.
Shinitzky, M., & Barenholz, Y. (1978) *Biochim. Biophys. Acta 515*, 367–394.
Slater, T. F. (1984) *Methods Enzymol. 105*, 283–293.
Straume, M., & Litman, B. J. (1987) *Biochemistry* (following paper in this issue).
Stubbs, C. D. (1983) *Essays Biochem. 19*, 1–39.
Stubbs, C. D., Kouyama, T., Kinosita, K., Jr., & Ikegami, A. (1981) *Biochemistry 20*, 4257–4262.
Stubbs, C. D., Kinosita, K., Jr., Munkonge, R., Quinn, P. J., & Ikegami, A. (1984) *Biochim. Biophys. Acta 775*, 374–380.
Stubbs, G. W., & Litman, B. J. (1978) *Biochemistry 17*, 220–225.
Stubbs, G. W., Litman, B. J., & Barenholz, Y. (1976) *Biochemistry 15*, 2766–2772.
Sunamoto, J., Baba, Y., Iwamoto, K., & Kondo, H. (1985) *Biochim. Biophys. Acta 833*, 144–150.
Thompson, T. E., & Huang, C. (1986) in *Physiology of Membrane Disorders* (Andrioli, T. E., Hoffman, J. F., Fanestil, D. D., & Schultz, S. G., Eds.) 2nd ed., pp 25–44, Plenum, New York.
van der Meer, W., Pottel, H., Herreman, W., Ameloot, M., Hendrickx, H., & Schroder, H. (1984) *Biophys. J. 46*, 515–523.
van de Ven, M., van Ginkel, G., & Levine, Y. K. (1984) *Biochem. Biophys. Res. Commun. 123*, 352–357.
Vogel, H., & Jahnig, F. (1985) *Proc. Natl. Acad. Sci. U.S.A. 82*, 2029–2033.
Vos, M. H., Kooyman, R. P. H., & Levine, Y. K. (1983) *Biochem. Biophys. Res. Commun. 116*, 462–468.
Wang, S., Glaser, M., & Gratton, E. (1986) *Biophys. J. 49*, 307a.
Wong, P. T. T. (1984) *Annu. Rev. Biophys. Bioeng. 13*, 1–24.
Yeagle, P. L. (1984) *Prog. Clin. Biol. Res. 159*, 153–175.
Yeagle, P. L., Hutton, W. C., Huang, C., & Martin, R. B. (1975) *Proc. Natl. Acad. Sci. U.S.A. 72*, 3477–3481.